Single-nucleon pickup spectroscopic factors for levels in ^{30}Si and ^{30}P and the D state of three-nucleon systems

C. M. Bhat, J. E. Bowsher, T. B. Clegg, H. J. Karwowski, and E. J. Ludwig
University of North Carolina at Chapel Hill, North Carolina 27514
and Triangle Universities Nuclear Laboratory, Durham, North Carolina 27706

B. A. Brown
Michigan State University, East Lansing, Michigan 48824
(Received 2 May 1988)

Angular distributions of differential cross sections and vector and tensor analyzing powers have been measured for transitions in ^{31}P(**d**,^{3}He)^{30}Si and ^{31}P(**d**,t)^{30}P reactions at $E_d \approx 16$ Mev. Exact, finite-range distorted-wave Born-approximation analyses have been performed using S- and D-state amplitudes for the three-nucleon systems. Calculations have also been carried out by incorporating realistic three-body wave functions. A j dependence in tensor analyzing powers observed for the first time in (d,^{3}He) and (d,t) reactions, can be reproduced in distorted-wave Born approximation calculations only by including a D-state amplitude for three-nucleon systems. We find that the tensor analyzing powers for $j = l_1 + \frac{1}{2}$ transfers exhibit significantly more pronounced D-state effects than those for $j = l_1 - \frac{1}{2}$ transfers. The analyzing powers along with the differential cross sections have been used to extract spectroscopic factors for the low-lying levels in ^{30}Si and ^{30}P, and the results have been compared with recent sd-shell-model predictions.

I. INTRODUCTION

Most previous experimental studies[1] of the spectroscopic factors for low-lying single-hole states in sd-shell nuclei have been made by measuring angular distributions of the differential cross section, and the analyses have employed the zero-range, distorted-wave Born-approximation (DWBA) formalism. For single-nucleon transfer reactions on a nucleus with nonzero ground-state spin, states in the final nucleus are often reached by more than one total angular momentum transfer j. It is difficult to extract spectroscopic factors corresponding to each j unambiguously by measuring angular distributions of cross sections alone. Yule and Haeberli[2] demonstrated the j dependence of vector analyzing powers (VAP) in single-nucleon transfer reactions. While cross-section angular distribution shapes for $j = l_1 + \frac{1}{2}$ and $j = l_1 - \frac{1}{2}$ transfer are similar, where l_1 is orbital angular momentum transfer to the target nucleus, two distinct patterns are obtained for vector analyzing powers. Hence, the analyzing power data become essential in establishing spectroscopic factors. Evidence for j dependence of tensor analyzing powers (TAP) has previously been observed[3,4] only in (**d**,p) reaction studies, and it has been shown[5] that this j dependence can be reproduced in DWBA calculations after inclusion of the deuteron D state.

In this paper we report on a study of low-lying levels in ^{30}Si and ^{30}P via the ^{31}P(**d**,^{3}He) and ^{31}P(**d**,t) reactions with a 16-MeV beam of vector- and tensor-polarized deuterons. Angular distributions of differential cross section $d\sigma/d\Omega$ and vector analyzing power A_y and tensor analyzing powers A_{xx} and A_{yy} have been measured, and spectroscopic factors have been deduced for a total of nine transitions. These spectroscopic factors are compared with recent sd-shell model calculations[6] which use a mass-dependent effective interaction and accurately predict single-particle level properties for nuclei near shell closure. Our goal is to provide a more stringent test of these calculations by comparing the model predictions with measured spectroscopic factors for nuclei in the middle of the sd-shell-model space. We have also investigated the j dependence of TAP resulting from D-state amplitudes in the ^{3}He and triton and have made a decomposition of $j = l_1 \pm \frac{1}{2}$ spectroscopic factors using the j dependence of VAP and TAP.

Previously the ^{31}P(**d**,^{3}He)^{30}Si reaction has been studied by Brown *et al.*[7] using vector polarized deuterons, and the separation of projectile and ejectile spin-orbit distortions in the ground-state transition has been investigated. However, they measured only relative cross sections and hence did not report spectroscopic factors. The study of ^{30}P by the ^{31}P(**d**,t) reaction is presented completely here for the first time. A new determination of D-state amplitudes in three-nucleon systems using only our data for the ground-state transitions in ^{31}P(**d**,^{3}He)^{30}Si and ^{31}P(**d**,t)^{30}P reactions (which are dominated by $l_1 = 0$ transfer) has recently been reported.[8]

II. EXPERIMENTAL PROCEDURE

Experiments were performed at the Triangle Universities Nuclear Laboratory using the Lamb-shift polarized ion source.[9] The momentum analyzed vector and tensor polarized deuteron beam was focused on a target at the center of a 62-cm scattering chamber. The target was

made of 116-μg/cm^2 thick red phosphorus on a 20-μg/cm^2 gold foil. The thickness of the phosphorus target was determined by measuring Rutherford scattering cross sections with 4.4- and 5.0-MeV α particles, and agrees within 10% with the result obtained by an optical-model analysis of 16-MeV deuteron elastic scattering on the same target. The outgoing d, ^{3}He, and t have been detected using three symmetrically placed pairs of ΔE-E solid-state detectors arranged as telescopes and separated by 10° on each side of the incident beam direction. Typical pulse height spectra for ^{31}P(**d**,^{3}He)^{30}Si and ^{31}P(**d**,t)^{30}P reactions are shown in Fig. 1. Energy resolutions of 70 to 120 keV for ^{3}He and 60 to 70 keV for triton spectra have been obtained.

Angular distributions of $d\sigma/d\Omega$, A_y, A_{xx}, and A_{yy} have been measured for three transitions in the ^{31}P(**d**,^{3}He)^{30}Si reaction at $E_d = 16.2$ MeV. Results were obtained also for ^{31}P(**d**,d)^{31}P and for six transitions in ^{31}P(**d**,t)^{30}P at $E_d = 16$ MeV. Data are shown in Figs. 2, 4, and 6–10. The TAP come from an eight-step measurement scheme.[10] Angular distributions of $d\sigma/d\Omega$ for transitions in ^{31}P(d,^{3}He)^{30}Si were also obtained in a separate measurement using an unpolarized beam.

The beam polarization was continuously monitored using a ^{3}He(**d**,p) polarimeter[10] located downstream of the scattering chamber. The spin direction of the deuterons from the polarized ion source was flipped periodically between up and down, and the beam's polarization was changed every two minutes using a nuclear-spin-filter.[11] The polarizations of the two states used were typically $p_z^{(1)} = p_{zz}^{(1)} = 0.60$ and $p_z^{(2)} = 0$, $p_{zz}^{(2)} = -1.20$ with an absolute error estimated $\lesssim 3.1\%$.[10] The absolute error in $d\sigma/d\Omega$ for the ^{31}P(**d**,^{3}He)^{30}Si reaction is estimated to be $\approx 10\%$, mainly arising from target thickness uncertainties. For the ^{31}P(**d**,t)^{30}P reaction, the total error in the $d\sigma/d\Omega$ is larger because measurements obtained with a polarized beam require that uncertainties from target thickness, analyzing power and beam polarization must be combined. Our errors in analyzing powers for both reactions arise from statistics and from uncertainties in incident beam polarizations.

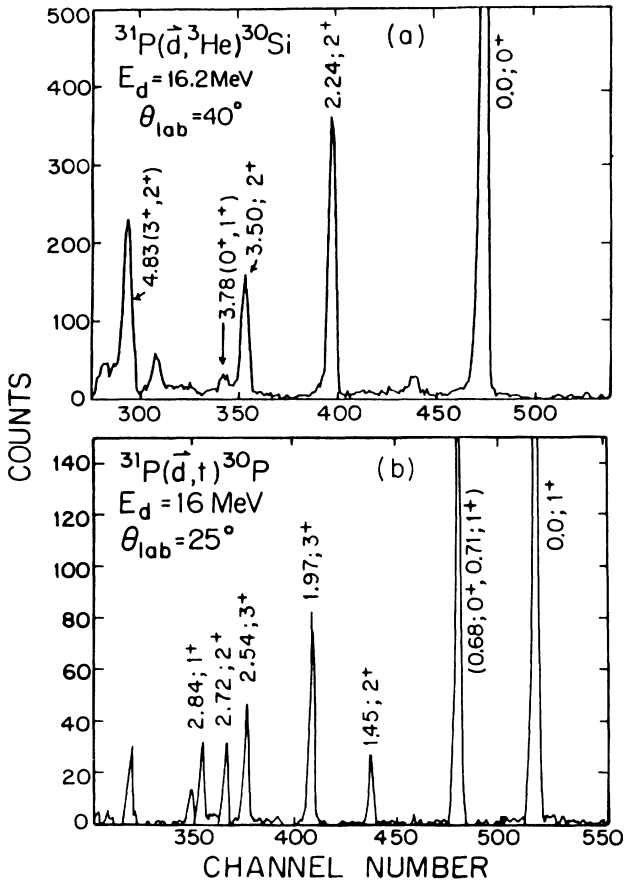

FIG. 1. Pulse height spectrum for (a) ^{31}P(**d**,^{3}He)^{30}Si reaction at $E_d = 16.2$ MeV and (b) ^{31}P(**d**,t)^{30}P reaction at $E_d = 16$ MeV.

III. DWBA ANALYSIS

A. DWBA theory and the D state of the three-nucleon system

The DWBA transition amplitude for a direct, one-step $A(d,t)B$ reaction is given by,[12,13]

$$T_{td} = \int X_f^{*(-)}(k_t r_t) \langle B,t \mid V_{dn} \mid d, A \rangle X_i^{(+)}(k_d r_d) d\tau \quad (1)$$

where, X_i and X_f^* are optical model wave functions corresponding to the initial and final channels respectively, and are obtained from elastic scattering studies. Here V_{dn} is the interaction potential between the neutron and deuteron determined from the triton binding energy. For a (d,^{3}He) reaction the DWBA formalism is similar except that quantities for the triton and neutron are replaced by those for the ^{3}He and proton, respectively. The single-nucleon-pickup spectroscopic amplitudes for levels in the final nucleus enter the DWBA transition amplitude [Eq. (1)] by a parentage expansion of the wave function of target nucleus A,

$$\Phi_A(J_A, M_{J_A}) = \sum_{j, l_1, J_B} \beta_{jl_1}(J_A, J_B)[\Phi_B(J_B, M_{J_B})\phi(j, l_1)]_{J_A} . \quad (2)$$

Here, Φ_B and ϕ are the wave functions of nucleus B and the single nucleon, respectively. The quantity β_{jl_1} is the single-nucleon spectroscopic amplitude, which can be predicted by shell model calculations.

The differential cross section and analyzing powers are expressed in terms of the DWBA transition amplitudes.[12,13] It has been shown that predicted TAP are very sensitive to the detailed structure of the triton.[14,15] This structure appears in the transition amplitude through the matrix element $\langle d,n \mid V_{dn} \mid t \rangle$, which is given by

$$\langle d,n \mid V_{dn} \mid t \rangle = B_{td} \langle d,n \mid t \rangle - T_{\text{kin}} \langle d,n \mid t \rangle . \quad (3)$$

Here, B_{td} is the binding energy difference between the triton and deuteron, and T_{kin} is kinetic energy operator for the triton. The overlap integral $\langle d,n \mid t \rangle$ in terms of S and D states of relative motion between the deuteron and single-nucleon is[15]

$$\langle d,n \mid t \rangle = \sqrt{4\pi} \sum_{l_2=0,2} \sum_{\lambda,\sigma} u_{l_2}(r) Y^{\lambda}_{l_2}(r)(l_2 \lambda s \sigma \mid 1/2\sigma_t) \times (1/2\sigma_n 1\sigma_d \mid s\sigma) \quad (4)$$

where s is the spin transfer. Here l_2 is the relative deuteron-neutron orbital angular momentum in the triton. For the triton S state $l_2=0$ and $s=\frac{1}{2}$, and for the D state $l_2=2$ and $s=\frac{3}{2}$. In the Clebsch-Gordan coefficient in Eq. (4), λ, σ, σ_d, σ_n, and σ_t are projection quantum numbers for the angular momentum vectors $\mathbf{l}_2$,$\mathbf{s}$, and spins of deuteron, neutron and triton, respectively. The radial motion of the neutron relative to the deuteron is given by $u_{l_2}(r)$. The TAP arise from interference between S- and D-state amplitudes and hence are expected to be sensitive to the D state of the triton. The relative importance of the D-state amplitude to that of the S state in a DWBA analysis for (d,t) reactions at low energies depends mainly[14–16] on the asymptotic D/S-state ratio η, where

$$\eta = \lim_{r\to\infty} \frac{u_2(r)}{u_0(r)} . \quad (5)$$

An additional parameter, D_2, is defined by

$$D_2 = \frac{1}{15} \frac{\int u_2(r) r^4 dr}{\int u_0(r) r^2 dr} \quad (6)$$

and is related to η by an approximate and model-dependent relation $D_2 \approx \alpha^{-2}\eta$, where $\alpha^2 = 2\mu B_{td}/\hbar^2$ and μ is the reduced mass. Calculations made using separable interactions[16] showed that the relation between η and D_2 for the three-nucleon system holds to within 5%. There have been a number of theoretical[16,17] and experimental[8,18–20] determinations of the D_2 and/or η parameter(s) for the ^{3}He and triton. Recent theoretical estimates for both three-nucleon systems based on a realistic Hamiltonian predict $D_2 = -0.223$ fm^2 (Ref. 16) and -0.23 fm^2 (Ref. 17). These are comparable to experimentally deduced values of $D_2(^3\text{He}) = -0.24 \pm 0.04$ fm^2 and $D_2(t) = -0.25 \pm 0.05$ fm^2 (Ref. 8). In this work we use the latter values of D_2 for the ^{3}He and triton for determining spectroscopic factors[12] $S = (N+1)\beta^2_{jl_1}$ in exact, finite-range DWBA analyses, where N is number of active nucleons in the target. All DWBA analyses have been carried out using the computer code TWOFNR.[21]

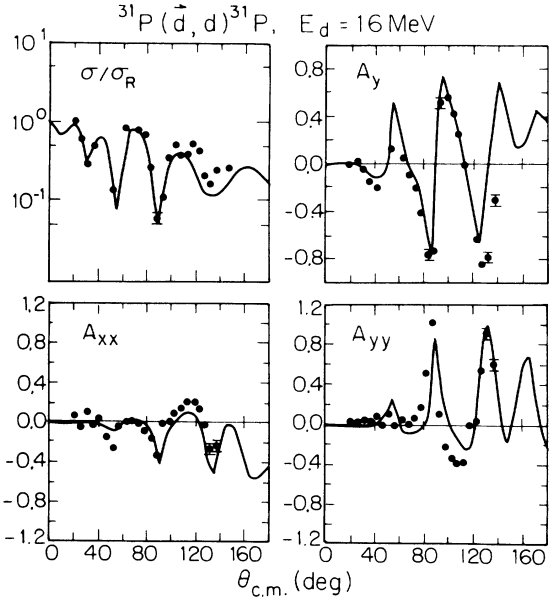

FIG. 2. Elastic scattering observables for the ^{31}P(**d**,d)^{31}P reaction at $E_d = 16$ MeV. The curves correspond to an optical model fit with the parameter set given in Table I.

B. Optical model potential parameters

The deuteron optical model potential (OMP) parameters used in the DWBA calculations for ^{31}P(**d**,^{3}He)^{30}Si and ^{31}P(**d**,t)^{30}P reactions have been obtained from optical model analyses of 16-MeV elastic scattering of a vector- and tensor-polarized deuteron beam from ^{31}P. Starting with a deuteron global OMP from Ref. 22, searches for the best-fit OMP parameter set used measured angular distributions of $d\sigma/d\Omega$ and A_y. Resulting OMP parameters also gave satisfactory agreement with our (**d**,d) TAP data. The optical model calculations were performed using the computer code OPTICS.[23] No effort was made to include tensor potentials in this optical model analysis. It was shown by Takei *et al.* that measured angular distributions of T_{22} and T_{20} in deuteron elastic scattering on various nuclei can be explained without them.

Figure 2 shows the result of best-fit optical model calculations for the ^{31}P(**d**,d)^{31}P data. The extracted OMP parameters are given in Table I along with those for the ^{3}He and triton, taken from Ref. 25. The value of $r_{s.o.}$ obtained here for deuteron elastic scattering is slightly

TABLE I. Optical model potential parameters (notation from Ref. 26) used in the present DWBA calculations.

Channel	V_0 (MeV)	r_0 (fm)	a_0 (fm)	W_V (MeV)	W_D (MeV)	r_W (fm)	a_W (fm)	$V_{s.o.}$ (MeV)	$r_{s.o.}$ (fm)	$a_{s.o.}$ (fm)
d[a]	95	1.144	0.73		12.2	1.325	0.749	5.3	0.75	0.55
^{3}He[b]	160	1.16	0.71	28.0		1.38	0.92	14.5	1.04	0.25
t[b]	160	1.12	0.68	31.7		1.28	0.95	7.2	0.96	0.25

[a]The best-fit parameters from the present ^{31}P(**d**,d) elastic scattering.
[b]Parameters from Ref. 25.

smaller than the one used in Ref. 7. However, detailed DWBA analyses for the ^{31}P(d,^{3}He)^{30}Si and ^{31}P(d,t)^{30}P reactions showed that the spectroscopic factors are the same (within 2%) for $r_{s.o.}$ values increased by 30%. To check on the sensitivity to ^{3}He and triton parameters, other DWBA analyses have been carried out by replacing parameters from Ref. 25 with the global ^{3}He and triton OMP parameters of Becchetti and Greenlees.[26] Spectroscopic factors obtained using the two sets of OMP parameters agree within 5%.

C. Bound-state wave functions

The single-nucleon, radial form factors at the target vertex [i.e., radial part of $\phi(j,l_1)$ in Eq. (2)] have been generated in a Woods-Saxon potential well with geometry parameters determined from electron-scattering studies.[27] Well depths were adjusted to match the experimental single-nucleon separation energies from the target nucleus.

For radial form factors at the projectile (triton or ^{3}He) vertex [i.e., $u_{l_2}(r)$ in Eq. (4)], one uses the two-body form factor corresponding to relative motion between the deuteron and a nucleon in the three-body system. Two methods exist for constructing such a two-body form-factor. The most common for heavier systems is the nucleon separation-energy method; alternatively here, one can use realistic three-body wave functions projected onto a two-body system.

In the separation-energy procedure, where the nucleon is bound in a potential well (Woods-Saxon or Gaussian), the potential depth is adjusted to reproduce the binding energy of the nucleon with the deuteron. For the Woods-Saxon (WS) potential, a radius parameter $r_0=1.5$ fm and a diffuseness parameter $a_0=0.5$ fm have been suggested.[28] This set of geometry parameters gives a range parameter[28] $\beta=1.5$ fm^{-1} and rms radii of 2.75 and 2.69 fm for the ^{3}He and triton, respectively. The normalized wave functions for $l_2=0$ and 2, obtained by solving the Schrödinger equation, are weighted by appropriate S and D-state amplitudes of Ref. 8 to get $u_0(r)$ and $u_2(r)$. The solid curves shown in Fig. 3 are the single-nucleon form factors corresponding to this Woods-Saxon potential which are used in the finite-range DWBA calculations.

In the alternative procedure for form-factor calculation we used two different, recent three-body wave functions selected from the literature, which predict similar values of the D_2-parameter. Gibson and Lehman[16] (GL) have calculated the overlap integrals, $\langle d,n \mid t \rangle$ by solving Faddeev equations in momentum space for various values of deuteron D-state probabilities, P_D, in the range of 0% to 10%, and list $u_{l_2}(k)$, where k is the momentum vector. The dashed curves shown in Fig. 3 were calculated with wave functions corresponding to $P_D=7\%$, and have been obtained by making a Fourier transformation[16] using

$$u_{l_2}(r)=\sqrt{1/\pi}\int_0^\infty j_{l_2}(kr)k^2u_{l_2}(k)dk\ , \tag{7}$$

where $j_l(kr)$ are the spherical Bessel functions. The third set of wave functions have been obtained by using realistic two-body and three-body interactions. Schiavilla, *et al.*[17] (SPW) evaluated $\langle d,p \mid {}^3\mathrm{He} \rangle$ ($\approx\langle d,n \mid t \rangle$) by a variational method for three different types of interactions. The form factors corresponding to the Argonne + Model-VII–type interaction[17] are shown by dotted curves in Fig. 3. Even though the asymptotic behavior of the three wave functions (WS, GL, and SPW) is similar, they differ considerably for $r \lesssim 4$ fm.

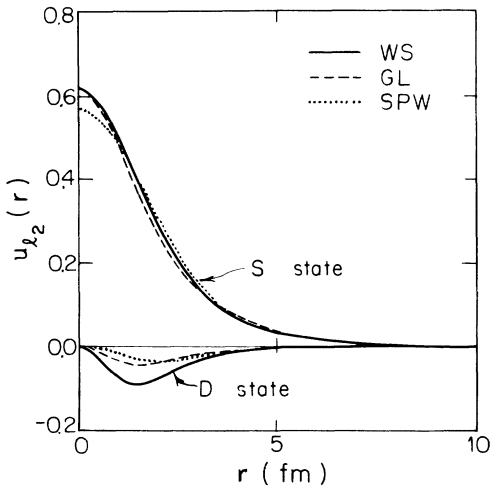

FIG. 3. A comparison of form factors $u_{l_2}(r)$. The solid curve corresponds to a Woods-Saxon potential (WS) and a D-state form factor with $D_2=-0.24$ fm^2. The dashed curve is the Gibson-Lehman (GL) wave function (Ref. 16) with deuteron D-state probability $P_D=7\%$. The dotted curves are wave functions of Schiavilla *et al.* (SPW) corresponding to the Argonne + Model-VII interaction (Ref. 17).

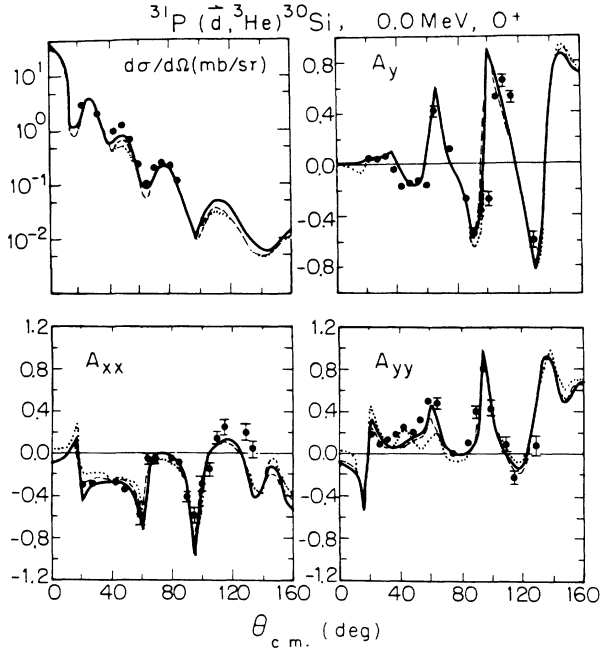

FIG. 4. Comparison of exact, finite-range DWBA analyses for the ground-state transition in the ^{31}P(d,^{3}He)^{30}Si reaction at $E_d=16.2$ MeV using form factors shown in Fig. 3. The solid, dashed and dotted curves correspond to analogous curves in Fig. 3.

Figure 4 gives a comparison of DWBA calculations made for the ground state transition in the ^{31}P(d,^{3}He)^{30}Si reaction using these three form factors. We find the predictions for cross section, A_y and A_{xx} to be in rather good agreement with the data for all three wave functions, but for A_{yy} the data indicate a preference for WS or GL predictions over those of SPW. Detailed DWBA calculations made for the ^{31}P(d,t)^{30}P(0.0 MeV, 1^+) transition produce similar results. No effort was made to include GL or SPW wave functions for any excited states because most of these involve mixed j transfer. This fact, plus our higher experimental uncertainties for the excited states precluded using them to help distinguish between GL or SPW wave functions. Present DWBA analyses for all transitions were performed using form factors obtained by the separation-energy procedure.

D. Sensitivity of TAP to D-state amplitudes, and j dependence

Considerable theoretical and experimental effort[18,19] has been extended to determine the D-state admixtures in three-nucleon systems by exploiting the sensitivity of TAP to the D-state amplitude. Previously we determined D_2 (and η) parameters for the ^{3}He and triton using the transitions for which $2s_{1/2}$ pickup is dominant.[8] Cases illustrating sensitivity of TAP to D-state amplitudes of the triton are shown in Fig. 8. From this it is clear that the DWBA calculations give a good description of the data only when the D-state amplitude is included.

To investigate the j dependence of TAP in (d,^{3}He) and/or (d,t) reactions, systematic DWBA calculations were made with the transferred j corresponding successively to different shell-model orbits. The points in Fig. 5 were obtained by calculating TAP as a function of j transfer. In that figure the quantity

$$\delta=\sum[\{\mathrm{TAP}(S+D)-\mathrm{TAP}(S)\}\Delta\theta]^2$$

provides a measure of the differences in TAP calculated

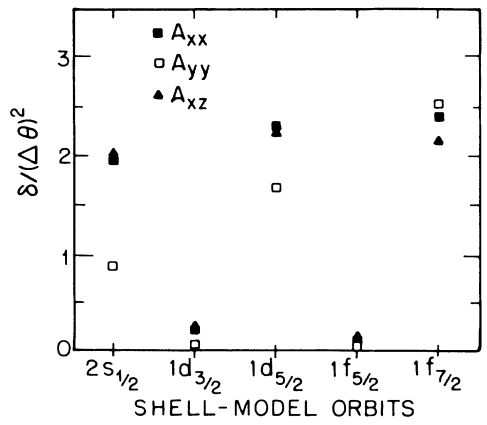

FIG. 5. The sensitivity of predicted TAP to the transferred j in a (d,^{3}He) reaction. The DWBA calculations were performed with S- and D-state amplitudes ($D_2=-0.24$ fm^2). The quantity δ is defined in the text. The solid, open, and triangular points are obtained for A_{xx}, A_{yy}, and A_{xz}, respectively, $\Delta\theta=5°$.

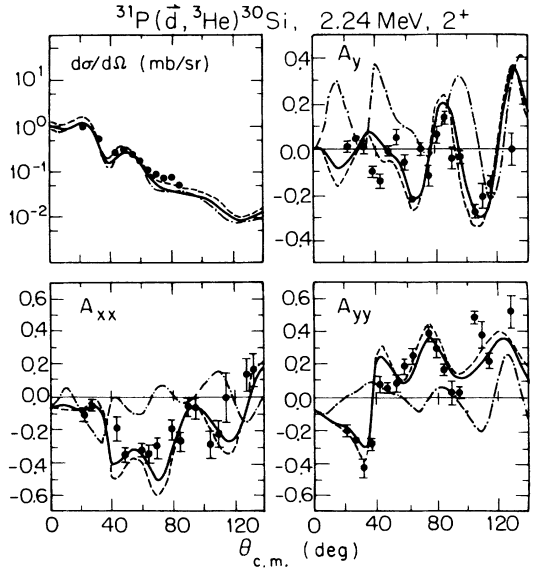

FIG. 6. Angular distributions for the $d\sigma/d\Omega$, A_y, A_{xx}, and A_{yy} for the 2.24-MeV level excited in the ^{31}P(d,^{3}He)^{30}Si reaction at $E_d=16.2$ MeV. The solid curve results from an exact, finite-range DWBA analysis using the best-fit spectroscopic factors. Dashed and dash-dot curves are obtained assuming pure $1d_{5/2}$ and $1d_{3/2}$ pickup, respectively. All curves are obtained by including S- and D-state amplitudes for ^{3}He with $D_2(^3\mathrm{He})=-0.24$ fm^2. The DWBA cross-section curves for $1d_{3/2}$ and $1d_{5/2}$ pickup are arbitrarily normalized to the experimental data.

by including first S- and D-state amplitudes ($D_2=-0.24$ fm^2), and then the S-state amplitude alone. The summation is made over the angular range of 0° to 180° with an angular step $\Delta\theta=5°$. The solid, open and triangular points are for A_{xx}, A_{yy} and A_{xz}, respectively. Similar results have been obtained for the ^{32}S(d,^{3}He)^{31}P reaction.[29] Interestingly, the effect of D-state amplitude on TAP for $j=l_1+\frac{1}{2}$ transfers is more pronounced than for $j=l_1-\frac{1}{2}$ transfers. We also find that the D-state effect becomes more pronounced as l_1 increases. Previously, similar observations were made only for (d,p) reactions.[19]

A theoretical explanation of such j dependence of the TAP for a (d,p) reaction was given by Santos.[5] The present investigation reveals similar results for (d,^{3}He) or (d,t) reactions. The dash-dot and dashed curves of Fig. 6 result from DWBA calculations for $l_1=2$, $j=\frac{3}{2}$ and $\frac{5}{2}$ pickup, respectively, in the ^{31}P(d,^{3}He)^{30}Si reaction including the S- and D-state amplitudes with $D_2=-0.24$ fm^2. Two distinct patterns of angular distributions are obtained for $j=l_1+\frac{1}{2}$ and $j=l_1-\frac{1}{2}$ transfers. For example, the angular distribution of A_{xx} for $1d_{5/2}$ pickup has a wide negative dip with a minimum $A_{xx}\approx-0.6$ at angles near 70°, while A_{xx} for $1d_{3/2}$ pickup is oscillatory with smaller amplitude excursions from zero. A systematic investigation extended to the $1f_{7/2}$ and $1f_{5/2}$ shell shows similar distinct features. A comparison of angular distributions of A_{xx} for $j=l_1+\frac{1}{2}$ for different l_1 values showed a characteristic angular shift of the centroid of the first wide minimum. Thus, for the (d,^{3}He)

and (d,t) reactions a distinct j dependence of TAP is seen in the presence of the D-state amplitude for the three-nucleon system. This j dependence makes TAP a useful observable for nuclear spectroscopy. Hence, the TAP can be employed along with VAP in determining relative spectroscopic factors whenever different j transfers are possible in a given transition.

IV. SPECTROSCOPIC FACTORS

A. ^{31}P(d,^{3}He)^{30}Si reaction

The data for three low-lying levels studied here are compared with the results of finite-range, DWBA calculations in Figs. 4, 6, and 7. Starting from shell-model predictions,[6] the spectroscopic factors were varied to give a best fit to the data. The solid curves in these figures represent these best fits. For transitions with mixed j transfer, spectroscopic factors corresponding to each j have been determined by analytically minimizing

$$X^2=\sum_{i=1}^{n}\left[\frac{E_i-T_i}{\Delta_i}\right]^2$$

by a technique similar to the method adopted in Ref. 30. Here E_i are experimental observables ($d\sigma/d\Omega$, VAP, or TAP), T_i are the corresponding theoretical values, n comprises all of the data points, and Δ_i is the experimental statistical error for each data point. The T_i are deduced from calculated angular distributions of $d\sigma/d\Omega$, VAP, or TAP for the two allowed j transfers added incoherently after weighting each with the corresponding spectroscopic factor.

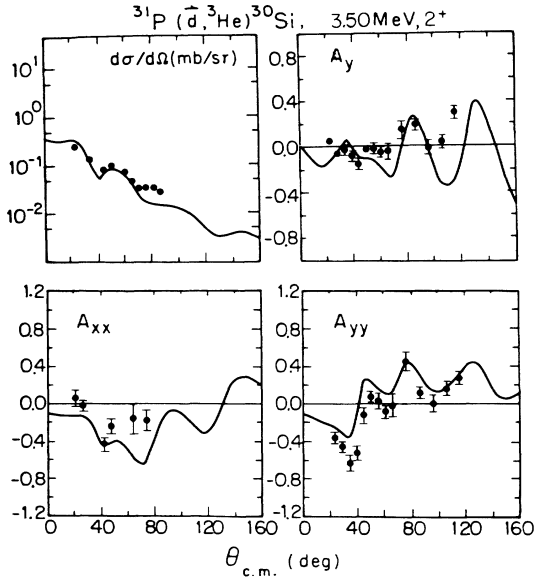

FIG. 7. Angular distributions for $d\sigma/d\Omega$, A_y, A_{xx}, and A_{yy} for the 3.50-MeV levels excited in ^{31}P(d,^{3}He)^{30}Si reaction at $E_d=16.2$ MeV. The solid curves have the same significance as in Fig. 6.

Data are generally well reproduced by the DWBA calculations. A comparison of the present spectroscopic factors with those of previous single-particle transfer reaction studies[31] and with the sd-shell model predictions[6] is given in Table II. For the ground state transition, which is a pure j transfer, the spectroscopic factor is predicted very well by the sd-shell model calculations. For this and other pure j transfers errors in spectroscopic factors are estimated to be 15% due mainly to target thickness uncertainty. Spectroscopic factors for the 2.24-MeV (2^+) level from the compilation in Ref. 31 are somewhat larger than those from present measurement. Previously, Mackh *et al.*[32] attempted to decompose spectroscopic factors for $1d_{3/2}$ and $1d_{5/2}$ pickup to this state using the j dependence of the cross section angular distribution; they inferred a larger $1d_{3/2}$ pickup strength than that for $1d_{5/2}$. In contrast, we find a larger $1d_{5/2}$ strength. An illustration of the decomposition of $1d_{3/2}$- and $1d_{5/2}$-pickup strengths is presented for the 2.24-MeV transition in Fig. 6. From the angular distribution of differential cross section alone one cannot draw firm conclusions, while the VAP and TAP show striking differences between $1d_{3/2}$ and $1d_{5/2}$ pickup. By similar decomposition for the 3.50-MeV (2^+) level we find larger $1d_{5/2}$-pickup strength than obtained in Ref. 32. The decomposition of spectroscopic factors for $j=l_1\pm\frac{1}{2}$ is feasible when the analyzing powers are also used. Hence, the present results offer more rigorous tests of the nuclear model calculations.

A summed spectroscopic factor[33] for single-nucleon pickup from the $2s_{1/2}$ shell is predicted by the sd-shell model calculations[6] to be 1.33 for the levels below 10-MeV excitation in ^{30}Si. However, in this study only about 60% of the total strength is seen implying that the missing strength should appear in excited states above 3.5 MeV. The $\sum S$ of our measured spectroscopic factors for $1d_{3/2}$ and $1d_{5/2}$ pickup are respectively 0.43 and 2.37, while sd-shell-model predictions[6] are 0.38 and 1.42. Hence, the shell-model calculations[6] appear to underestimate spectroscopic factors for the $1d_{5/2}$ shell.

B. ^{31}P($\bar{d}$,t)^{30}P reaction

In this study six low-lying levels of ^{30}P have been investigated. For all these levels the angular distributions of $d\sigma/d\Omega$, A_y, and A_{yy} have been measured. Only for the ground state and for the doublet around 0.7 MeV (in the present measurement the 0.68-MeV, $J^\pi=0^+;T=1$ and 0.71-MeV, $J^\pi=1^+;T=0$ states are not resolved) were angular distributions of A_{xx} also extracted. Experimental data and comparison with DWBA predictions are shown in Figs. 8–10. The spectroscopic factors measured here are compared with sd-shell-model predictions and with the compilation of Endt[31] in Table II.

Angular momentum selection rules for transitions to 1^+ levels in ^{30}P allow $l_1=0$ and $l_1=2$. For the ground state, DWBA calculations using the shell-model spectroscopic amplitudes[6] underestimate the cross section, and the measured A_y show deeper minima than predicted.

TABLE II. Single-nucleon pickup spectroscopic factors for the low-lying levels of ^{30}Si and ^{30}P by ^{31}P(**d**,^{3}He)^{30}Si and ^{31}P(**d**,t)^{30}P reactions measured around 16 MeV are compared with previous experimental results and the predictions from full *sd*-shell-model calculations.

			Spectroscopic factors										
						Previous work							
	E_x		Present work[a]			c		d		$(E_x)_{th}$	*sd*-shell-model calculations[b]		
Reactions	(MeV)	J^π	$1d_{5/2}$	$2s_{1/2}$	$1d_{3/2}$	$l_1=0$	$l_1=2$	$l_1=0$	$l_1=2$	(MeV)	$1d_{5/2}$	$2s_{1/2}$	$1d_{3/2}$
^{31}P(**d**,^{3}He)^{30}Si	0.0	0^+		0.77		0.75±0.08		0.62		0.0		0.77	
	2.24	2^+	1.40		0.38		2.6±0.6		0.51+0.86[e]	2.31	0.83		0.38
	3.50	2^+	0.97		0.05		0.8±0.4		0.41+0.06[e]	3.55	0.59		0.0
		$\sum S$[f]	2.37	0.77	0.43					$\sum S$[f]	1.42	0.77	0.38
^{31}P(**d**,t)^{30}P	0.0	1^+		1.0		0.66±0.12	0.12±0.04	0.62	0.13	0.0		0.56	0.07
	0.68	$0^+;1$[g]		0.77		0.75±0.08		0.74		0.68		0.77	
	0.71	1^+[g]		0.09	0.25			0.11	0.46	0.64		0.09	0.25
	1.45	2^+	(0.3)[h]		(0.1)[h]		0.47±0.10		0.57	1.49	0.05		0.28
	1.97	3^+	0.75				0.75±0.13		0.76	2.06	0.65		
	2.54	3^+	0.75				0.65±0.10		0.69	2.51	0.45		
	2.72	2^+	0.44		0.07		0.47±0.095		0.77	2.46	0.33		0.02
		$\sum S$[f]	2.24	1.09	0.42					$\sum S$[f]	1.48	0.65	0.62

[a]The errors in spectroscopic factors for the ground-state and transitions with pure j transfers in ^{31}P(**d**,^{3}He)^{30}Si and ^{31}P(**d**,t)^{30}P reactions are typically 15%, which mainly arise from the target thickness normalization. For states with mixed j-transfers the errors are higher because of uncertainties in establishing j admixtures and poorer statistics. The uncertainties are estimated to be 20% unless otherwise specified.

[b]Reference 6 provides a description of the model for these calculations.

[c]Reference 31. These are sums for isoscalar transitions.

[d]From Ref. 32 for the ^{31}P(**d**,^{3}He)^{30}Si reaction and Ref. 34 for the ^{31}P(**d**,t)^{30}P reaction; they quote C^2S, where C is the isospin Clebsch-Gordan coefficient. $C^2=2/3$ for transitions in the ^{31}P(**d**,^{3}He)^{30}Si reaction studied here and $C^2=1$ for transitions in the ^{31}P(**d**,t)^{30}P reaction except for the 0.69-MeV ($J^\pi=0^+, T=1$) transition.

[e]From Ref. 32 $S=0.51+0.86$ represents individual spectroscopic factors for $1d_{5/2}$ shell as 0.51 and for $1d_{3/2}$ shell as 0.86. Similar notation is used for 3.5-MeV level. Decomposition of spectroscopic factor in both cases is based on cross-section angular distribution.

[f]Reference 33.

[g]Here the 0.68- and 0.71-MeV levels are not resolved. Hence, we used shell-model amplitudes from Ref. 6 in our DWBA calculations.

[h]Obtained by best visual fit; X^2 minimization does not give acceptable fit to the data and these values of spectroscopic factors are highly uncertain by $\approx 50\%$.

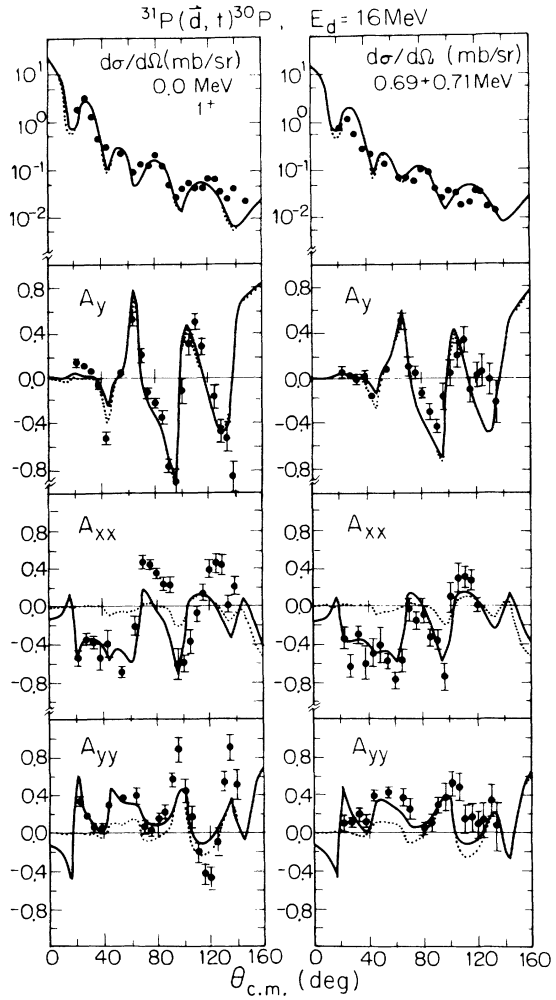

FIG. 8. Angular distributions for $d\sigma/d\Omega$, A_y, A_{xx}, and A_{yy} for the ground state and 0.68 + 0.71-MeV levels excited in ^{31}P(d,t)^{30}P reaction at $E_d = 16$ MeV. The curves result from exact, finite-range DWBA calculations including the S and D states for the triton with $D_2(t) = -0.25$ fm^2. For the ground-state transition, spectroscopic factors determined in the present study have been used, while for the 0.68 + 0.71-MeV levels, the amplitudes from Ref. 6 have been used. The dotted curves in both cases were obtained with only an S-state amplitude for the triton.

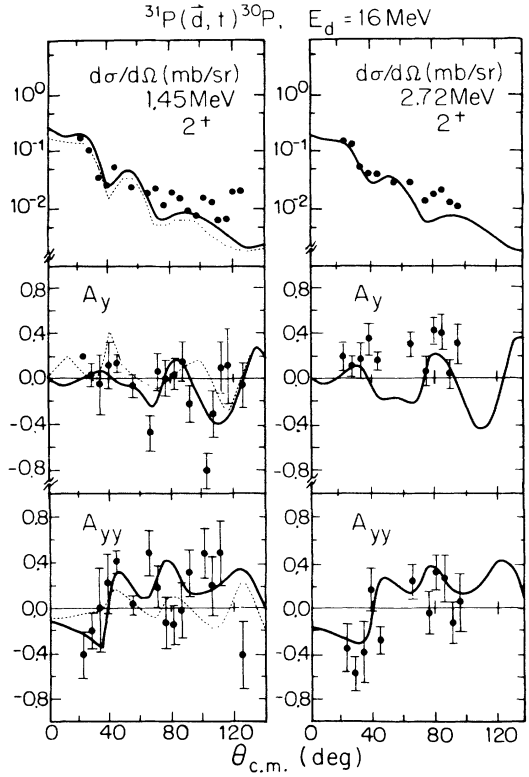

FIG. 9. Angular distributions for $d\sigma/d\Omega$, A_y, and A_{yy} for the 1.45- and 2.72-MeV levels with $J^\pi = 2^+$, excited in the ^{31}P(d,t)^{30}P reaction at $E_d = 16$ MeV. The curves were obtained with spectroscopic factors determined in the present study. The dotted curve in case of 1.45-MeV transition is obtained by using predicted spectroscopic amplitudes from Ref. 6.

The data suggests a spectroscopic factor of 1.0, which is slightly larger than previous measurements.[1,31,34]

The 0.68-MeV level is the isobaric analogue of the ground state in ^{30}Si excited in the ^{31}P(d,^{3}He) reaction. Since the resolution in the present study was not adequate to resolve this state from the 0.71-MeV level, we cannot determine spectroscopic factors for these levels. DWBA calculations made using the predicted[6] spectroscopic amplitude corresponding to the 0.68-MeV transition showed that the dominant contribution ($\approx$70%) in the peak at 0.68 + 0.71-MeV excitation in ^{30}P arises from the 0.68-MeV transition alone. The curves in Fig. 8 for the 0.68 + 0.71-MeV levels were obtained using the shell-model-predicted amplitudes.[6]

For 2^+ levels, the shell-model allows both $1d_{3/2}$ and $1d_{5/2}$ pickup. Hence, we tried to determine spectroscopic factors by fitting as explained in Sec. IV A whenever possible. Previous single-nucleon pickup[34] and stripping[35] reaction studies and sd-shell-model calculations[6] as well suggested dominant $j_1 = 2, j = \frac{3}{2}$ transfer for the lowest 2^+, 1.45-MeV level in ^{30}P. The shape of angular distribution of $d\sigma/d\Omega$ is very well predicted by $1d_{3/2}$ *or* $1d_{5/2}$ pickup. The analyzing powers, in particular A_{yy}, suggest a dominant $1d_{5/2}$ pickup as shown in Fig. 9. We find that $1d_{3/2}$ and $1d_{5/2}$ pickup spectroscopic factors of 0.1 and 0.3, respectively, provide best agreement with experimental data. However, experimental errors are large and agreement with calculations is sufficiently poor so that we cannot claim significant disagreement with shell-model calculations for this case. The dotted curve in Fig. 9 for the 1.45-MeV level is obtained by using sd-shell-model[6] spectroscopic amplitudes. For the 2^+ level at 2.72-MeV excitation, both our measurements and the sd-shell-model calculations[6] suggest a dominant $1d_{5/2}$ pickup.

The 1.97- and 2.54-MeV levels are known[1] to be $J^\pi = 3^+$, and the sd-shell model allows pure $1d_{5/2}$ pickup. Though the shapes of the cross section angular distributions are reproduced well by DWBA calculations the

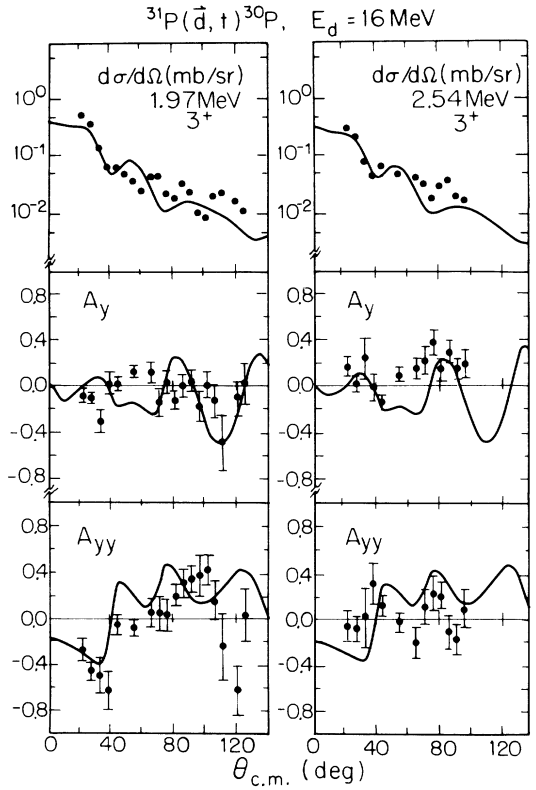

FIG. 10. Angular distributions for $d\sigma/d\Omega$, A_y, and A_{yy} for the 1.97- and 2.54-MeV, $J^\pi=3^+$ levels excited in the ^{31}P(**d**,t)^{30}P reaction at $E_d=16$ MeV. The curves have the same significance as in Fig. 9.

analyzing powers do not agree well. Spectroscopic factors obtained here are in good agreement with previous measurements.[31,34]

From Table II, it can be seen that $\sum S$ for $2s_{1/2}$ pickup is 1.09, and a dominant fraction of this strength is exhausted by the ground state alone. However, the *sd*-shell model[6] predicts a total $2s_{1/2}$-pickup strength of 0.86 for the levels below 10.0-MeV excitation in ^{30}P. For the same excitation energy range a total strength of 2.43 is predicted[6] for the $1d_{5/2}$ shell and about 60% of this strength (i.e., $\sum S=1.48$) should be exhausted by the levels below 2.72-MeV excitation. However, the present measurement gives $\sum S=2.24$ for the $1d_{5/2}$ shell.

V. SUMMARY AND CONCLUSIONS

We have measured angular distributions of $d\sigma/d\Omega$, VAP, and TAP for a total of nine transitions in ^{31}P(**d**,^{3}He)^{30}Si and ^{31}P(**d**,t)^{30}P at $E_d=16$ MeV. The OMP parameters for the entrance channel were obtained by an optical model analysis of elastic scattering of 16-MeV vector- and tensor-polarized deuterons on ^{31}P. Exact finite-range DWBA analyses were performed using the *S*- and *D*-state amplitudes for three-nucleon systems. In general the shapes of the angular distributions of differential cross section and analyzing power data for the transitions in the ^{31}P(**d**,^{3}He)^{30}Si reaction are well explained by the one-step DWBA. For low-lying transitions involving $2s_{1/2}$ and $1d_{3/2}$ proton transfers there is excellent agreement between measured and *sd*-shell-model spectroscopic factors. Theory appears to underestimate the $1d_{5/2}$ strength, however. In the case of the ^{31}P(**d**,t)^{30}P reaction, DWBA predictions are less satisfactory for the 1.97- and 2.54-MeV levels, both having $J^\pi=3^+$ and predominant $1d_{5/2}$ strengths.

Using the present (d,^{3}He) data we could not distinguish clearly between different three-body wave functions obtained from realistic nucleon-nucleon interactions. We find that DWBA predictions of TAP with the GL wave function compare marginally better with the measured data than those predicted with the SPW wave function. However, angular distribution shapes for cross section and vector analyzing power are similar for all three types of wave functions used here.

An attempt has been made to study the j dependence of TAP in (d,^{3}He) and (d,t) reactions. We believe that clear evidence for the j dependence of TAP has been observed. This can be reproduced in DWBA calculations only by including a *D*-state amplitude for the three-nucleon system. Hence, TAP can also be used with angular distributions of cross section and VAP to establish angular momentum transfer and spectroscopic factors for single-nucleon transfer reactions. In the present work, decomposition of spectroscopic factors for transitions involving mixed-j transfers has been achieved using the j dependence of vector- and tensor-analyzing powers whenever possible. Finally, calculations show that TAP for $j=l_1+\frac{1}{2}$ transfers are more sensitive to *D*-state effects than those for $j=l_1-\frac{1}{2}$ transfers. Therefore, TAP for *pure* $j=l_1+\frac{1}{2}$ transitions in (d,^{3}He) and (d,t) reactions should be very useful in establishing *D*-state amplitudes in three-nucleon systems.

ACKNOWLEDGMENTS

The authors would like to thank D. J. Abbott, R. E. Fauber, T. M. Mooney, and T. C. Spencer for their help during data taking. We acknowledge valuable discussions with W. J. Thompson, D. R. Lehman, and A. M. Eiró, and thank Y. Aoki for providing the recent version of TWOFNR. This research was partially supported by the U.S. Department of Energy, Office of High Energy and Nuclear Physics, under Contract No. DE-AS05-76ER02408.

[1]P. M. Endt and C. van der Leun, Nucl. Phys. A **310**, 1 (1978).
[2]T. J. Yule and W. Haeberli, Phys. Rev. Lett. **19**, 756 (1967).
[3]L. D. Knutson, E. J. Stephenson, N. Rohrig, and W. Haeberli, Phys. Rev. Lett. **31**, 392 (1973).
[4]A. K. Basak, J. A. R. Griffith, O. Karban, J. M. Nelson, and S. Roman, Nucl. Phys. A **295**, 111 (1978).
[5]F. D. Santos, Phys. Rev. C **13**, 1145 (1976).
[6]B. H. Wildenthal, *Progress in Particle and Nuclear Physics,* edited by D. Wilkinson (Pergamon, Oxford, 1984), Vol. 11, p. 5.
[7]J. D. Brown *et al.*, Nucl. Phys. A **436**, 125 (1985).
[8]C. M. Bhat, T. B. Clegg, H. J. Karwowski, and E. J. Ludwig, Phys. Rev. C **37**, 1358 (1988).
[9]T. B. Clegg, G. A. Bissinger, and T. A. Trainor, Nucl. Instrum. Methods **120**, 445 (1974).
[10]S. Tonsfeldt, Ph.D. thesis, University of North Carolina at Chapel Hill, 1980, available from University Microfilms.
[11]J. L. McKibben, G. P. Lawrence, and G. G. Ohlsen, Phys. Rev. Lett. **20**, 1180 (1968).
[12]N. K. Glendenning, Ann. Rev. Nucl. Sci. **13**, 191 (1963).
[13]G. R. Satchler, *Direct Nuclear Reactions* (Clarendon, Oxford, 1983).
[14]F. D. Santos, A. M. Eiró, and A. Barroso, Phys. Rev. C **19**, 238 (1979).
[15]R. C. Johnson and F. D. Santos, Part. and Nucl. **2**, 285 (1974).
[16]B. F. Gibson and D. R. Lehman, Phys. Rev. C **29**, 1017 (1984).
[17]R. Schiavilla, V. R. Pandharipande, and R. B. Wiringa, Nucl. Phys. A **449**, 219 (1986).
[18]T. E. O. Ericson and M. Rosa-Clot, Ann. Rev. Nucl. Part. Sci. **35**, 271 (1985).
[19]L. D. Knutson and W. Haeberli, Prog. Part. Nucl. Phys. **3**, 127 (1982).
[20]I. Sick, in *The Three-Body Force in Three-Nucleon System,* Vol. 260 of *Lecture Notes in Physics,* edited by B. L. Berman and B. F. Gibson (Springer-Verlag, Berlin, 1986), p. 42; B. Vuaridel *et al.*, *ibid.*, p. 281.
[21]M. Toyoma and M. Igarashi, TWOFNR (unpublished).
[22]W. W. Daehnick, J. D. Childs, and Z. Vrcelj, Phys. Rev. C **21**, 2253 (1980).
[23]R. J. Eastgate, W. J. Thompson, and R. A. Hardekopf, Comp. Phys. Commun. **5**, 69 (1973).
[24]M. Takei, Y. Aoki, Y. Tagishi, and K. Yagi, Nucl. Phys. A **472**, 41 (1987).
[25]R. A. Hardekopf, R. E. Brown, F. D. Correll and G. G. Ohlsen, *Polarization Phenomena in Nuclear Reactions, Sante Fe, 1980,* edited by G. G. Ohlsen *et al.* [Am. Phys. Soc. Conf. Proc. **69**, 496 (1980)].
[26]F. D. Becchetti and G. W. Greenlees, *Polarization Phenomena in Nuclear Reactions,* edited by H. H. Barschall and W. Haeberli (University of Wisconsin Press, Madison, Wisc., 1971), p. 629.
[27]J. Street *et al.*, J. Phys. G **8**, 839 (1982).
[28]A. M. Eiró (private communication).
[29]C. M. Bhat, E. J. Ludwig, T. B. Clegg, and H. J. Karwowski (unpublished).
[30]N. J. Davis and J. M. Nelson, Nucl. Phys. A **468**, 357 (1987).
[31]P. M. Endt, At. Data Nucl. Data Tables **19**, 23 (1977).
[32]H. Mackh, G. Mairle and G. M. Wagner, Z. Phys. **269**, 353 (1974).
[33]P. J. Brussaard and P. W. M. Glaudemans, *Shell-model Applications in Nuclear Spectroscopy* (North-Holland, Amsterdam, 1977).
[34]J. J. M. Van Gasteren, A. J. L. Verhage, and A. Van der Steld, Nucl. Phys. A **231**, 425 (1974).
[35]W. W. Dykoski and D. Dehnhard, Phys. Rev. C **13**, 80 (1976).